Photoelectron Spectroscopy of the Rare Gases*

James A. R. Samson and R. B. Cairns
Experimental Physics Laboratory, GCA Corporation, Bedford, Massachusetts
(Received 22 April 1968)

A spherical retarding potential analyzer was used to measure the kinetic energies of electrons ejected by photo-ionization of the rare gases as a function of wavelength from the $^2P_{1/2}$ ionization threshold down to about 400 Å. The ratio of the number of ions produced in the ground $^2P_{3/2}$ state to the number produced in the excited $^2P_{1/2}$ state was found to be constant with respect to wavelength and had the following values: 2.18, 1.98, 1.79, and 1.60 for Ne, Ar, Kr, and Xe, respectively. From these data the specific photo-ionization cross sections for the rare gases were obtained. At wavelengths shorter than the M_1, N_1, and O_1 thresholds for Ar, Kr, and Xe, respectively, the ejection of s electrons was observed and the specific cross sections for their production measured.

INTRODUCTION

The study of the kinetic energies of photoelectrons ejected from gaseous atoms and molecules by vacuum ultraviolet radiation is relatively new. This study has been named photoelectron spectroscopy.[1] Work in this field was first described by Vilesov *et al.*[2] in 1961 and independently by Turner[3] in 1962. Photoelectron spectroscopy has been used to determine higher ionization potentials of molecules, specific photo-ionization cross sections, Franck-Condon factors, and relative electronic transition probabilities.[4]

Briefly, the principle of the method is as follows. In the photo-ionization process a photon of energy $h\nu$ will eject an electron with a specific energy. The residual ion will also be given some energy. However, since momentum is conserved the energy partition between the electron and the ion is in the inverse ratio of their masses. Therefore, practically all of the energy is carried away by the electron. Thus the energy E_j of a particular photoelectron is given by

$$E_j = h\nu - I_j , \tag{1}$$

where $h\nu$ represents the photon energy and I_j represents the jth ionization potential of the atom or molecule. Therefore, knowledge of both the electron and photon energies is sufficient to give the ionization potential of the atom or molecule. If the number of electrons n_j of energy E_j and the total number of electrons $n_0 = \Sigma_j n_j$ are measured then the specific photo-ionization cross section σ_j for producing an ion in the jth state is given by

$$\sigma_j = (n_j/n_0)\ \sigma_t , \tag{2}$$

where σ_t is the total photo-ionization cross section. Most electron energy analyzers cannot measure the total number of photoelectrons ejected and simply sample a fraction of these electrons. If this fraction is constant for all energy groups the ratio n_j/n_0 will be unaltered and the analyzer can be used to measure specific cross sections, relative transition probabilities, and Franck-Condon factors.

Several types of electron energy analyzers can be used such as retarding potential, magnetic deflection, or electrostatic deflection analyzers. For the work reported here a spherical retarding potential analyzer was used, similar in principle to that reported by Frost *et al.*[5] The apparatus and experimental problems are discussed in the next section, while the specific photo-ionization cross sections for Ne, Ar, Kr, and Xe are given in the final section.

EXPERIMENTAL TECHNIQUES

In order to obtain meaningful values of the ratio n_j/n_0 it is essential either that the analyzer does not discriminate against electrons of different energies or that the magnitude of such discrimination be known. One cause of discrimination common to most analyzers is the possibility that photoelectrons photoelectrons for polarized radiation has the general form $A + B\cos^2\theta$, where θ is the angle of ejection relative to the electric vector of the incident radiation.[6,7] In general, electrons ejected from different shells (different j values) and electrons of different energies will have different values of the coefficients A and β. Thus it is desirable to accept electrons over as large a cone angle about the electric vector as possible to minimize discrimination caused by different angular distributions. The angular distributions of photoelectrons from Ar, Kr, and Xe have been measured by Berkowitz *et al.*[8,9] at 584 Å and by Chaffee[10] for potassium at 2400 Å. In each case an outer-shell electron was removed. Theoretically, it is predicted that $A = 0$ for an s electron thus the electron should have an angular distribution proportional to $\cos^2\theta$. Chaffee has shown this to be the case for ejection of a 4s electron from potassium. Berkowitz has shown that the angular distribution of p electrons ejected from Xe is nearly proportional to $\cos^2\theta$, but in Kr and Ar the angular distribution is successively more isotropic.

A further complication arises if the degree of polarization of the incident radiation varies with wavelength. If this is the case the angular distribution of the photoelectrons will also vary with wavelength. Thus it is necessary to know the degree of polarization of the radiation causing ionization. The degree of polarization produced by the monochromator used in the present work was measured at wavelengths between 400 Å and 900 Å by the method of Rabinovitch *et al.*[11]; see Fig. 1.

Further discrimination may be caused by electron

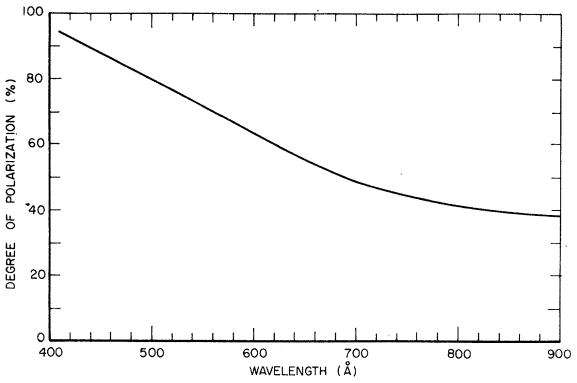

FIG. 1. Degree of polarization as a function of wavelength of radiation emerging from a one-half meter Seya monochromator equipped with a 1200-line/mm gold-coated grating.

collisions with the gas atoms under investigation. Brode has shown that these collisional cross sections depend strongly on the energy of the electrons.[12] The presence of this type of discrimination was checked by measuring the ratio of the total electron current to the intensity of the transmitted radiation. This ratio is proportional to the total photo-ionization cross section when the gas pressure is sufficiently low that no attenuation of the incident beam is observable. When this ratio is measured as a function of wavelength and suitably normalized it should reproduce the absolute value of the total photo-ionization cross-section curves obtained previously.[13] Any deviation gives a quantitative measure of the discrimination and thereby provides the appropriate correction factor. This type of discrimination existed in the present apparatus, its magnitude varying with pressure.

A schematic diagram of the analyzer is shown in Fig. 2. It consisted of three concentric spherical grids with a variable retarding potential applied to the middle grid. The diameters of the spheres were 3, 4, and 5 in. Two hollow metal tubes at the same potential as the inner sphere allowed radiation from the exit slit of a $\frac{1}{2}$-m Seya monochromator to enter the analyzer and release photoelectrons in the small volume element at the center of the spheres. The separation of the two tubes was was about 9.5 mm. Baffles in the first tube defined the light path so that no radiation struck the walls of the tubes, thereby causing a background of unwanted photoelectrons. The radiation emerging from the tubes was monitored by a photomultiplier sensitized to vacuum uv radiation with a coating of sodium salicylate. The photoelectrons produced at the center of the sphere traveled outwards along radii, i.e., in directions normal to the retarding potential. Electrons produced off center traveled at some angle to a radius and were retarded at a lower voltage. The relative diameters of the volume element and the inner sphere therefore set a limit to the resolving power of the analyzer. With the chosen dimensions, electrons of energy E should have had an energy spread $\Delta E/E = (1.56 \pm 0.1)\%$. The measured resolution of the

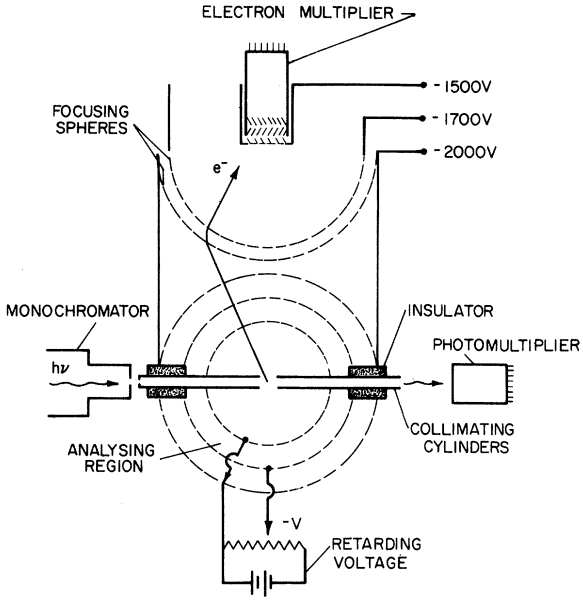

FIG. 2. Spherical-grid retarding potential electron energy analyzer.

analyzer was 1.65% for electron energies in excess of 4 eV. For lower energies the total energy spread tended to a constant value of $\Delta E = 56$ mV. That is, in terms of a full width at half-height, structure separated by 28 mV could be observed. However, this resolution could be achieved only when a Helmholtz coil was used to reduce the Earth's magnetic field from 0.5 G to about 0.05 G. The energy spread ΔE of the analyzer is shown in Fig. 3 as a function of the electron energy. The dotted line indicates the expected spread in energy caused by the finite dimensions of the apparatus. The deviation from this expected value may have been caused by small contact potentials in the field free

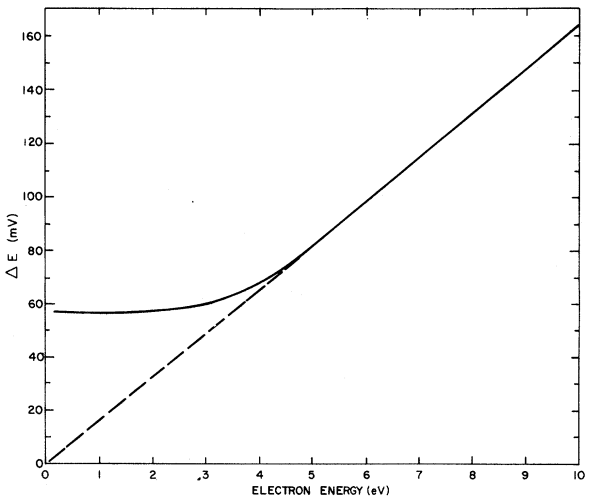

FIG. 3. Total energy spread ΔE of the electron energy analyzer as a function of electron energy.

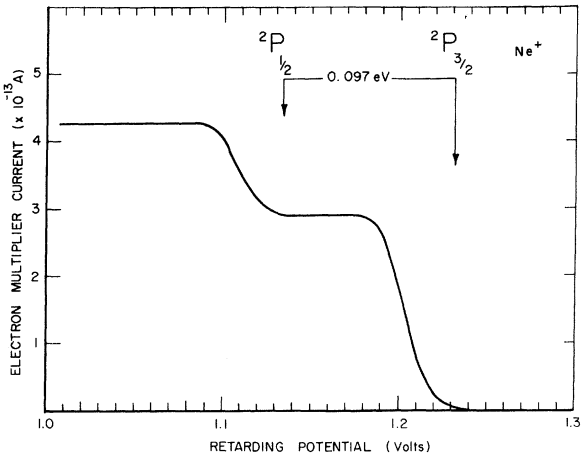

FIG. 4. Retarding potential curve for Ne ionized by 543.884 Å.

region where the electrons were created or by weak fields penetrating the holes of the mesh. Brass mesh with thirty holes per inch was used in constructing the spheres.

Electrons which escaped from the analyzer within a cone of 60° centered at right angles to the incident radiation were intercepted by a spherical mesh electrostatic lens[14] and focused onto the first dynode of an electron multiplier. Since the electron multiplier was used in the dc mode, the entire analyzer had to be held at about 2000 V negative to ground. The gas within the analyzer was maintained at pressures less than 5×10^{-3} Torr to prevent high-voltage arcing within the electron multiplier.

As the retarding potential of the analyzer was increased, a series of steps in the electron current appeared as each electron energy group was completely retarded. This is illustrated in Fig. 4 where the retarding potential curve is shown for neon photo-ionized by radiation of 543.884 Å. At this wavelength neon can be ionized into either the ground $^2P_{3/2}$ state [with ionization potential (I. P.) = 21.564 eV] or the excited $^2P_{1/2}$ state (I.P. = 21.661 eV). Thus two groups of electrons should appear separated by 97 mV. The ratio of the numbers of electrons within each group is a measure of the relative transition probabilities for producing these two states of ionized neon. From Fig. 4 it can be seen that these two states were clearly resolved with the ground-state ion 2.18 times more abundant than the excited ion. The energy spread in the retarding potential steps was 56 mV.

RESULTS

To obtain the specific photo-ionization cross sections of the rare gases as a function of wavelength it was only necessary to produce retarding potential curves such as that shown in Fig. 4 and measure the ratio of the step heights. Equation (2) can be rewritten for the case of the two electron groups producing the $^2P_{1/2,\,3/2}$ states of the rare-gas ions as follows:

$$\sigma_{3/2}=\sigma_t R/(1+R);\quad \sigma_{1/2}=\sigma_t/(1+R), \tag{3}$$

where $\sigma_{3/2}$ and $\sigma_{1/2}$ denote the specific cross sections for producing ions in the $^2P_{3/2}$ and $^2P_{1/2}$ states, respectively, and R is the ratio of the two-step heights, namely, $n_{3/2}/n_{1/2}$. From Eq. (3) it can be seen that $R=\sigma_{3/2}/\sigma_{1/2}$. Measured values of this ratio for Ne, Ar, Kr, and Xe plotted against the energy of the $^2P_{1/2}$ electron are given in Fig. 5. Each datum point was the average of several measurements. The error to be associated with each datum point was dependent on the signal to noise ratio but nowhere exceeded ±6%. Within the limits of experimental error the ratio was constant for a given atom. Similar results have been obtained by Comes and Sälzer for Ar, Kr, and Xe but over a smaller wavelength range.[15] However, near the $^2P_{1/2}$ threshold Comes and Sälzer obtained very large values of the ratio. This was undoubtedly caused by discrimination of the lower-energy electron group. Similar results have been observed in the present work when contact potentials were present in the field-free region of the analyzer where the electrons were created. It was possible to correct for this discrimination by using the calibration technique discussed in the previous section. The results of Comes and Sälzer are compared with the present work in Table I. Several other investigators have measured these ratios at the 584.3-Å helium resonance line using different types of analyzers.[5,16] Their results are also compared with the present values in Table I. Berkowitz *et al.*[9] quote a ratio of 1.93±0.1 for Kr at 584.3 Å. Villarejo *et al.*[17] have also studied the electron energies from Ar, Kr, and Xe. However, their technique consisted of measuring the number of electrons ejected at a fixed energy as the wavelength of the photo-ionizing radiation was varied. The fixed energy was chosen to be almost zero thus they could study threshold events. Their ratio measurements gave the number of ions in the $^2P_{3/2}$ state at that threshold wavelength (1022.1 Å for Xe) to the num-

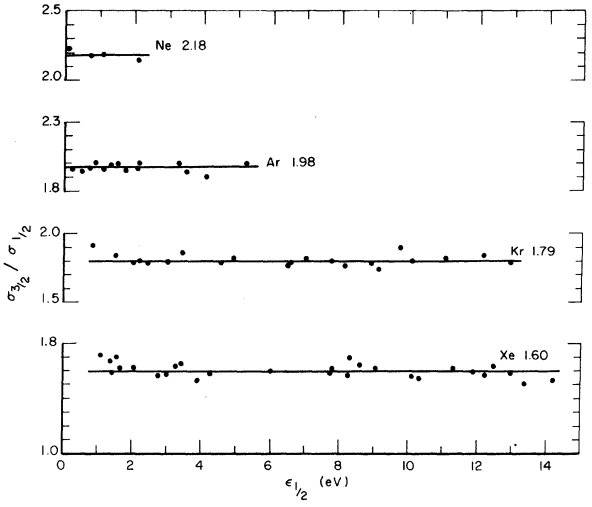

FIG. 5. Ratio of the abundances of ions produced in their $^2P_{3/2}$ and $^2P_{1/2}$ states measured as a function of the excess energy $\epsilon_{1/2}$ beyond the $^2P_{1/2}$ edge.

TABLE I. The ratio $\sigma_{3/2}/\sigma_{1/2}$ of the specific photo-ionization cross sections for producing ions in their $^2P_{3/2}$ and $^2P_{1/2}$ states.

Gas	Present work	Turner and May[a]	Frost *et al.*[b]	Comes and Sälzer[c]
Ne	2.18	...	...	...
Ar	1.98	...	1.96	2.14
Kr	1.79	1.79	1.73	1.69
Xe	1.60	1.69	1.68	1.66

[a]D. W. Turner and D. P. May, J. Chem. Phys. 45, 471 (1966).
[b]D. C. Frost, C. A. McDowell, and D. A. Vroom, Proc. Roy. Soc. (London) 296, 566 (1967).
[c]F. J. Comes and H. G. Sälzer, Z. Naturforsch. 19a, 1230 (1964).

ber of ions in the $^2P_{1/2}$ state at the corresponding threshold wavelength (922.8 Å for Xe). For Xe they obtained a value of 1.81. Knowing the total photo-ionization cross sections at these threshold wavelengths their ratio can be converted to the measured ratios given in Table I. A value of 1.58 is obtained for Xe in good agreement with the present work.

The ratios $\sigma_{3/2}/\sigma_{1/2}$ measured at a fixed wavelength were not simply related to the ratio of the statistical weights of the two states, which is 2 : 1. In general this remained true even if the ratio were computed at two different wavelengths chosen such that the energies of the ejected electrons were the same. In Xe for example, the ratio computed in this way was 1.73 : 1 near the $^2P_{1/2}$ threshold and increased to 2 : 1 at wavelengths shorter than 600 Å.

Applying the data from Fig. 5 to Eq. (3) and making use of the previously measured total photo-ionization cross sections[13] the specific photo-ionization cross sections of Ne, Ar, Kr, and Xe were obtained. The results are shown for each gas in Figs. 6–9, respectively. In the cases of Ar, Kr, and Xe a third group of electrons appeared when the gases were ionized by radiation of wavelengths shorter than the threshold for ejection of an *s* electron. The measured kinetic energies of these electrons identified them as *s* electrons from the outer subshells of the atoms. Because of the large energy differences between the *s* and *p* electrons corrections for energy discrimination had to be applied as discussed in the last section. This gave the number of *s* electrons produced to be approximately 4% of the total number of electrons. The accuracy of this result is poor because of the weakness of the signal. However, it is probably correct to within a factor of 2.

The correction applied above did not take into account the possible difference in angular distribution between the *s* and *p* electrons. Since the acceptance angle of the detector was fixed (60° cone) signals from electrons ejected in a directional manner were too large relative to signals from electrons ejected in a more isotropic fashion. This effect would be more pronounced if plane polarized radiation were used. From Fig. 1 it can be seen that radiation of wavelengths less than about 450 Å was nearly plane polarized. Thus, in the case of argon,

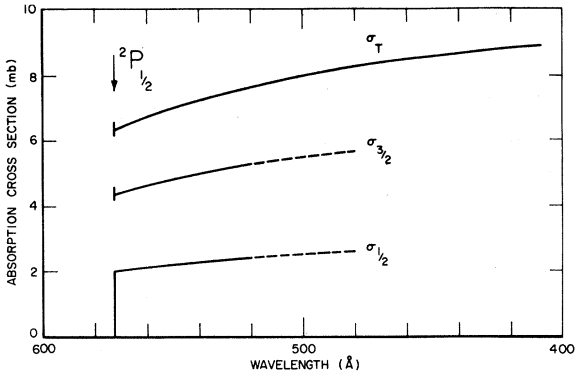

FIG. 6. Specific photo-ionization cross sections for Ne. The solid lines represent the experimental data while the dashed lines represent extrapolated specific cross sections assuming the ratio $\sigma_{3/2}/\sigma_{1/2}$ remains constant at shorter wavelengths.

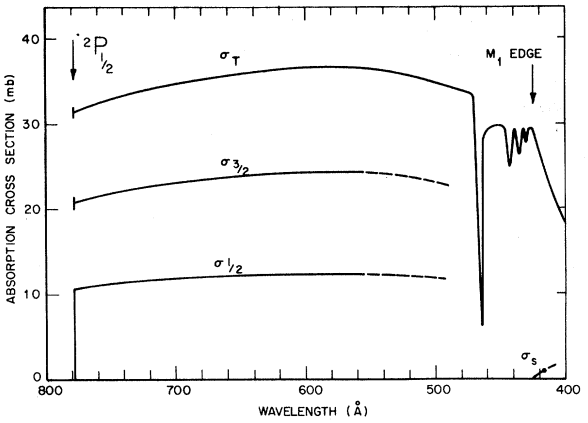

FIG. 7. Specific photo-ionization cross sections for Ar. The solid lines represent the experimental data while the dashed lines represent extrapolated specific cross sections assuming the ratio $\sigma_{3/2}\,\sigma_{1/2}$ remains constant at shorter wavelengths. The solid circle represents the cross section for ejection of an *s* electron.

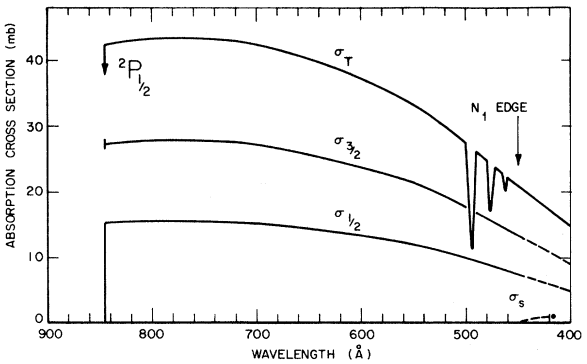

FIG. 8. Specific photo-ionization cross sections for Kr. The solid lines represent the experimental data while the dashed lines represent extrapolated specific cross sections assuming the ratio $\sigma_{3/2}\sigma_{1/2}$ remains constant at shorter wavelengths. The solid circle represents the cross section for ejection of an *s* electron.

the abundance of s electrons at 416 Å is expected to be less than the observed 4%. For the same wavelength Manson and Cooper[18] calculated the relative abundance of the s electrons to be of the order of 0.4%. Thus both experiment and theory indicate that the cross section near threshold for ejection of s electrons from the outer subshells of the rare gases is small compared with that for ejection of a p electron.

In Figures 7–9 several resonances are shown in the total cross-section curves. This structure can be correlated with the resonance series for excitation of an s electron discovered by Madden and Codling.[19] At the series limit no change in the cross section has been observed although energetically an s electron could be ejected. This can now be understood since in the original work[13] a change in cross section of less than 4% would not have been detected.

It is of interest to know the ratio $\sigma_{3/2}/\sigma_{1/2}$ within the resonances. For such measurements, a continuum radiation source would be desirable. However, with the discrete line source used in the present work, it was possible to obtain some preliminary information by the chance coincidence of three strong radiation source emission lines of Ne*IV* with resonances in Xe. The emission lines and corresponding resonances are listed in Table II

TABLE II. Coincidence between light source emission lines and resonances in Xe and the ratio $\sigma_{3/2}/\sigma_{1/2}$.

Ne*IV* emission lines (Å)	$\frac{\sigma_{3/2}}{\sigma_{1/2}}$	Xe absorption resonances[a] (Å)	Remarks[a]
558.595	1.46	558.78	weak asymmetric line
		544.18	weak window-type resonance
543.884	0.77	543.89	weak asymmetric line with the reduced absorption to the side of, and overlapping in the wings of, the 544.18 Å resonance.
		521.97	very weak and narrow (≈ 0.1 Å) window-type resonance
521.810 } 521.730 }	1.49	521.81	very weak and narrow (≈ 0.1 Å) window-type resonance

[a] R. Madden, K. Codling, and D. Ederer (private communication).

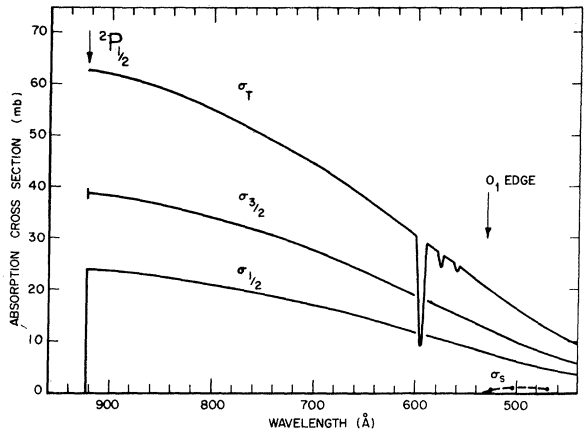

FIG. 9. Specific photo-ionization cross sections for Xe. The solid circles represent the cross sections for ejection of s electrons.

together with the value of the above ratio. The bracketed emission lines were of equal intensity[20] but unresolved with the present monochromator which was set for a band pass of 0.9 Å. The other lines were completely isolated. Hence the effective band pass was simply the width of the emission line produced in the light source. From previous measurements these linewidths were known to be typically 0.04 Å to 0.1 Å.[21] When the specific cross sections were calculated from the observed ratios it was found that the 558 Å and 521 Å resonances showed a decrease in the $\sigma_{3/2}$ cross section but no change in the $\sigma_{1/2}$ cross section. However, at the 543 Å resonance the $\sigma_{3/2}$ cross section decreased while the $\sigma_{1/2}$ cross section increased by almost the same magnitude. The net result was that the two large resonances practically annulled each other such that only a weak resonance could be observed in the total cross-section curve.

This type of information should be useful in calculating the degree of interaction between these resonances and the underlying continua. However, the present uncertainties of linewidth in both the light source lines and the absorption resonances make the calculation impractical at this time.

ACKNOWLEDGMENTS

We owe our thanks to Dr. Madden, Dr. Codling, and Dr. Ederer for permission to quote their data prior to its publication and to Dr. Frost for early discussions concerning spherical-grid retarding potential analyzers.

*This work has been supported by the National Aeronautics and Space Administration.

[1] M. I. Al-Joboury and D. W. Turner, J. Chem. Soc. 1963, 5141.

[2] F. I. Vilesov, B. L. Kurbatov, and A. N. Terenin, Dokl, Akad. Nauk. SSSR 138, 1329 (1961); 140, 797 (1961) [English transl.: Soviet Phys. – Doklady 6, 490 (1961); 6, 883 (1962)].

[3] D. W. Turner, J. Chem. Phys. 37, 3007 (1962).

[4] See, for example: M. I. Al-Joboury and D. W. Turner, J. Chem. Soc. 1967, 373; D. C. Frost, C. A. McDowell, and D. A. Vroom, Proc. Roy. Soc. (London) 296, 566 (1967); R. I. Schoen, J. Chem. Phys. 40, 1830 (1964); A. J. Blake and J. H. Carver, *ibid.* 47, 1038 (1967); J. A. R. Samson, Appl. Opt. 6, 403 (1967); R. Spohr and E. von Puttkamer, Z. Naturforsch. 22a, 705 (1967); J. Berkowitz, H. Ehrhardt, and T. Tekaat, Z. Physik 200, 69 (1967).

[5] D. C. Frost, C. A. McDowell, and D. A. Vroom, Phys. Rev. Letters 15, 612 (1965); Proc. Roy. Soc.

(London) 296, 566 (1967).
[6]H. A. Bethe and E. E. Salpeter, Quantum Mechanics of One- and Two-Electron Systems (Academic Press Inc., New York, 1957), p. 309.
[7]J. Cooper and R. N. Zare, J. Chem. Phys. 48, 942 (1968).
[8]J. Berkowitz and H. Ehrhardt, Phys. Letters 21, 531 (1966).
[9]J. Berkowitz, H. Ehrhardt, and T. Tekaat, Z. Physik 200, 69 (1967).
[10]M. A. Chafee, Phys. Rev. 37, 1233 (1931).
[11]K. Rabinovitch, L. R. Canfield, and R. P. Madden, Appl. Opt. 4, 1005 (1965).
[12]R. B. Brode, Rev. Mod. Phys. 5, 257 (1933).
[13]J. A. R. Samson, in Advances in Atomic and Molecular Physics, edited by D. R. Bates and I. Estermann (Academic Press Inc., New York, 1966), Vol. 2, p. 177.
[14]R. Reynolds and F. Scherb, Rev. Sci. Instr. 38, 348 (1967).
[15]F. J. Comes and H. G. Sälzer, Z. Naturforsch. 19a, 1230 (1964).
[16]D. W. Turner and D. P. May, J. Chem. Phys. 45, 471 (1966).
[17]D. Villarejo, R. R. Herm, and M. G. Inghram, J. Chem. Phys. 46, 4995 (1967).
[18]S. T. Manson and J. W. Cooper, Phys. Rev. 165, 126 (1968).
[19]R. P. Madden and K. Codling, Phys. Rev. Letters 10, 516 (1963); J. Opt. Soc. Am. 54, 268 (1964).
[20]C. E. Moore, Natl. Bur. Std. Circ. No. 488, Sec. 1 (1950).
[21]J. A. R. Samson and R. B. Cairns, J. Geophys. Res. 69, 4583 (1964).

Magnetic Hyperfine Structure of Lithium, Using an Approximate Projected Hartree-Fock Method*

Sten Lunell
Quantum Chemistry Group for Research in Atomic, Molecular, and Solid State Theory, Uppsala University, Uppsala, Sweden
(Received 15 March 1968)

An approximate projected Hartree-Fock calculation is performed for the ^2S ground state of the Li atom. It is shown that the use of general spin orbitals is essential for the treatment of the spin degeneracy in many-electron atoms. The energy obtained is -7.447536 a.u., which is lower than perviously published values obtained from s orbitals only. The value for the Fermi contact term is 2.846 a_0^{-3}, which is 97.9% of the experimental one. A natural spin-orbital analysis of the wave function is performed.

I. INTRODUCTION

The great majority of all quantum-mechanical calculations of atomic and molecular properties up to now have, except for the very simplest systems, been performed within the framework of the Hartree-Fock (HF) method or various approximations to it. The essential feature of all these methods is that the total wave function is approximated by a single (or occasionally a linear combination of) Slater determinant(s)

$$\Psi_0 = (N!)^{-1/2}\det|\,\psi_1(\vec{x}_1)\psi_2(\vec{x}_2)\cdots\psi_N(\vec{x}_N)|. \quad (1)$$

Here $\psi_i(\vec{x})$ is a one-particle wave function, and $\vec{x}_i$ denotes the three spatial coordinates and the spin coordinate of the electron i. This model has been very successful for many different types of problems and forms the conceptual framework for a large part of our physical thinking. There are cases, however, where it has failed quite remarkably. One such problem is the theory of magnetic hyperfine structure.

For S-state atoms the hyperfine splitting is given by the Fermi contact term.[1]

$$a_s = \tfrac{8}{3}\pi(\mu_n\mu_e/IJ)[\rho_+(0)-\rho_-(0)], \quad (2)$$

where μ_n and μ_e are the nuclear and electronic magnetic moments, respectively, I the nuclear spin, J the total electronic angular momentum, and $\rho_+(0)$ and $\rho_-(0)$ the $m_S=+\frac{1}{2}$ and $m_S=-\frac{1}{2}$ electron densities, respectively, at the nucleus. For the following it is convenient to introduce the Fermi contact parameter f,[2] defined by

$$f = 4\pi[\rho_+(0)-\rho_-(0)], \quad (3)$$

which does not involve any experimental quantities. For the ^2S ground state of Li a Hartree-Fock calculation gives the value $f=2.095$,[3] in poor agreement with the experimentally found f, which is 2.9062.[4] In other cases, e.g., the ^4S ground state of nitrogen, it even predicts zero splitting, contradictory to the experimental results.

II. THE SPIN-POLARIZED PHF METHOD

In the conventional Hartree-Fock method there are, besides the restriction to a single determinant, certain additional restrictions, of which we will list the most important ones.[5]

(i) The spin-orbitals $\psi_i(\vec{x})$ are assumed to be separable into a spatial part and a part only depending on the spin variable,